Kilogram Flash Joule Heating Synthesis with an Arc Welder

Lucas Eddy,[1,2] Jaeho Shin,[2] Yi Cheng,[2] Chi Hun Choi,[3] Carolyn Teng,[2] Phelecia Scotland,[3] Shichen Xu,[2] Alexander Lathem,[1,2] Shihui Chen,[2] Carter Kittrell,[2] Yimo Han,[3] and James M. Tour[1,2,3,4]*

[1]*Applied Physics Graduate Program and Smalley-Curl Institute,* [2]*Department of Chemistry,* [3]*Department of Materials Science and NanoEngineering,* [4]*The NanoCarbon Center and The Rice Advanced Materials Institute, and Department of Computer Science, Rice University, 6100 Main Street, Houston, Texas 77005, United States*

*Corresponding Author (Email: tour@rice.edu)

Key words: graphene, flash Joule heating, arc welder, carbon nanotubes, p-block metal dichalcogenides

Abstract Flash Joule heating has been used as a versatile solid-state synthesis method in the production of a wide range of products, including organic, inorganic, and ceramic products. Conventional flash Joule heating systems are large and customized, presenting significant barriers in the cost of assembly, the expertise needed to operate, and attaining uniformity of results between different systems. Even laboratory-scale flash Joule heating systems struggle to operate above 10-gram capacity, and they suffer poor temperature controllability. We present here the use of commercial off-the-shelf arc welders as a superior alternative to standard flash Joule heating systems due to their low cost ($120), ease of use, compact size, high temperature controllability, and tunability. We demonstrate gram-scale synthesis of a variety of organic and ceramic species using these systems. With the addition of a new reactor configuration for only $260, we scale up

synthesis of these products to record rates for laboratory scale, achieving a production rate of 3 kg/h for graphene, and kg/day production rates for SiC, carbon nanotubes, $SnSe_2$, and SnS_2.

1. Introduction

Flash Joule heating (FJH) is a technique by which electric current rapidly travels through a resistive medium, heating the sample on the millisecond to second timescale.[1] FJH has been used in a wide array of applications including solid state synthesis,[2,3] especially of graphene,[4] ceramics,[5] inorganics,[2,6] waste material upcycling,[7-11] and even soil remediation,[12] up to kilogram scales.[13] Conventional FJH uses a capacitor bank discharge to rapidly heat feedstocks up to or exceeding 3000 K. FJH systems are typically custom-designed, laboratory-made, and thus each system is often entirely unique.[1,13-15] These differences in FJH systems present a barrier to simple reproducibility across laboratories, since even small differences in system power, energy capacity, or time constant can significantly change the reaction heating profile.[16] Furthermore, the assembly of even gram-scale FJH systems often requires tens of thousands of dollars, personnel experienced in the assembly of high-voltage electrical equipment, and months of assembly prior to use.[17] Capacitor-based FJH systems feature comparatively low-temperature controllability,[1] are limited to reactions <10 s,[4] are difficult to scale cost-effectively, and can suffer damage to the system when the resistance of the feedstock is too low.[2] Finally, intense optimization work must be performed anew for every FJH system for every sample type and size in order to control reaction temperature within ~100 ºC,[18,19] such that optimization performed on one system does not easily translate to others.

We report here FJH, up to kilogram scales, using commercial off-the-shelf systems available for as low as $120. We use these systems as universal reactors to perform flash Joule and arc heating reactions to synthesize graphene, doped graphene, carbon nanotubes, carbyne, SiC, SnS_2, and $SnSe_2$. These commercial systems exhibit far superior temperature controllability relative to customized FJH systems and can be adjusted during a reaction. We achieve this using multiple models of arc welders, a variable transformer, and a programmable power supply. Multiple arc welders connected in series can also permit larger-scale reactions. We analyze the input energy use and output voltage, current, and power signals with microsecond resolution. We also highlight procedures enabling modification of these systems, including making a portable battery-powered FJH system that is recharged with portable commercial solar panels. These inexpensive and commercially available electrical sources are effective FJH systems, particularly in the synthesis of graphene up to kilogram scales, all done in the open air. This protocol renders Joule heating chemistry at the kilogram scale readily accessible to most any laboratory.

2. Results and Discussion

2.1 Synthesis of Flash Graphene with an Arc Welder

FJH reactions are commonly performed inside a tube reactor where the target feedstock is placed inside a fused quartz tube and between two graphite electrodes, which themselves are connected to the FJH system. Metallurgical coke (MC) is a commonly used feedstock in these reactors[1,13] for flash graphene (FG) synthesis due to its high carbon content, low monetary cost, and resistivity of ~0.01 Ω·m,[20] which translates to a resistance of ~1 Ω when packed into a FJH tube, commonly in 200 mg batches. The graphene resulting from conventional FJH is turbostratic in alignment, meaning that the layer stacking is disordered and thus exhibits a higher interlayer spacing relative

to ordered graphene. The previous use of this MC feedstock inspired the synthesis of metallurgical coke-derived flash graphene (MCFG) with an arc welder, as illustrated in **Figure 1**. A $120 DEKOPRO DKUS-MMA-160A arc welder (Amazon, **Figure 1a**) was used to heat 200 mg batches of MC using different arc welder settings. Electrical, thermal, and optical hazard safety procedures were followed during all reactions (**Figures S1-S2)**. The temperature of the reaction was measured using a Micro-Epsilon CTRM1H1SF100-C3 pyrometer at 1 ms resolution, with a minimum temperature threshold of 1000 ºC. The system current setting, which increases the electrical current output but does not correspond to the output in a 1:1 ratio, was adjusted in increments of 5 on the arc welder screen, resulting in an average temperature change of 35 ºC per the 5-increment adjustments (**Figure 1b**). This corresponds to temperature tunability on this system of 7 ºC/increment for this sample, which is very good control at these high temperatures. A sample of greater heat capacity would have correspondingly higher temperature tunability. Temperature control of this precision can be maintained during reactions even minutes in duration (**Figure S3**), although temperature-dependent sample resistance changes may require slight setting adjustments to maintain a constant temperature. This arc welder source is only slightly larger than a shoebox and weighs only 5.5 kg, underscoring the simplicity of arc welders as power sources. **Figure 1c** shows the changes in sample luminosity as a function of arc welder heating, and additional images are shown in **Figure S4.**

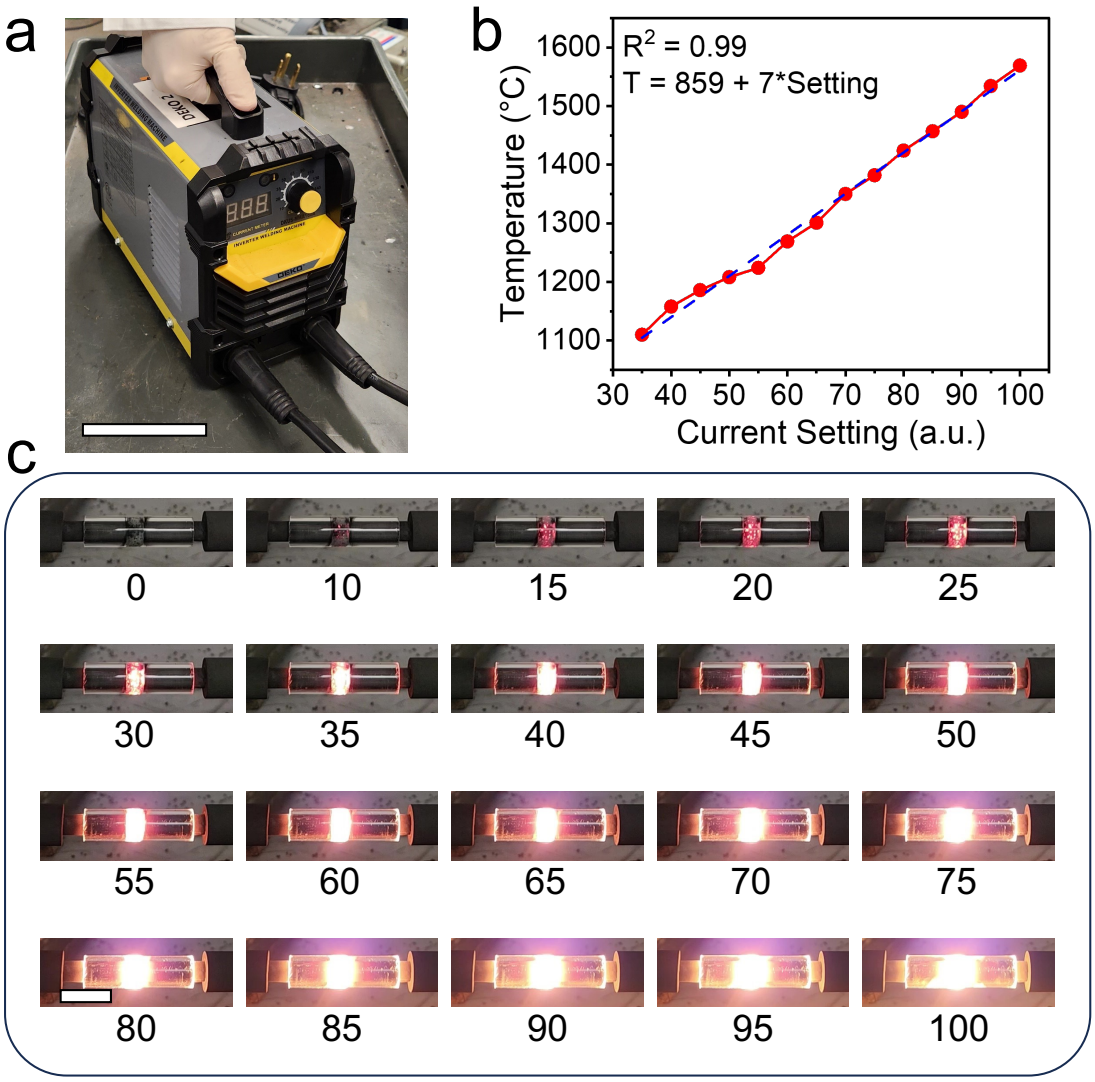

Figure 1. Performance of the DEKOPRO arc welder. a) Photo of DEKOPRO DKUS-MMA-160A arc welder. b) Temperature plotted as a function of the welder current output setting of 200 mg of MCFG. The arc welder was plugged into a 120 V outlet. MCFG was used for this measurement to avoid any heat contribution from the thermochemical transition from MC to MCFG. The current setting offers tunability at this scale of as little as 7 ºC/setting increment. The red dots illustrate the settings used in the experiment, and the blue dotted line illustrates the linear fit of the sample temperature plotted as a function of these settings. Each temperature increment was achieved after ~10 s of heating, relative to the previous increment. c) Image of 200 mg MC in an 8 mm inner

diameter quartz tube with graphite electrodes being heated by the DEKOPRO welder plugged into a 120 V outlet, which was used for all figures here, at the specified current output settings listed below each image. These current settings were read from the screen of the arc welder and correspond to the output current, but the setting displayed on the arc welder is not the current output in amperes, and hence these units are labeled as arbitrary units (a.u.). Scale bars, 10 cm (**a**); 2 cm (**c**).

2.2 Characterization of Arc Welder FG

Consistent with conventional FJH reactors, the quality of the FG produced corresponds to the input energy and power. This quality is evaluated in terms of turbostraticity, interlayer spacing, crystallinity, and defect density. Raman spectroscopy is one of the primary tools for bulk analysis of graphene. The Raman spectrum of FG exhibits a D peak at ~1360 cm^{-1}, which arises from defects in the graphene lattice or non-zigzag edges, a G peak at ~1600 cm^{-1}, which comes from the breathing modes of sp^2 carbon bonds,[19] and a 2D peak at ~2700 cm^{-1}, which has an intensity proportional to the crystallinity of graphitic layers and inversely proportional to the coupling between layers.[1,19,21] The intensities of the D and 2D peaks are often normalized by the intensity of the G peak, leading the peak intensity ratios, denoted $I_{D/G}$ and $I_{2D/G}$, to be considered quantitative values, where a lower $I_{D/G}$ indicates less defective graphene, and a higher $I_{2D/G}$ indicates better graphene conversion.[1] Conventionally, an $I_{2D/G}$ of at least 0.3 indicates graphene conversion.[19] **Figure 2a** illustrates the effects of different current settings on the FG product, using the DEKOPRO arc welder. The graphene yield can be monitored by investigating the emergence of the 2D peak. No FG is observed after reacting with a setting of 10, low FG yield with a setting of 50, and higher FG yield with a setting of 90, out of a maximum setting of 160. The long duration

of the reactions in comparison to those with capacitor-based FJH systems enables FG synthesis to occur well under 3000 ºC. The turbostratic character of graphene can be investigated by using a high-duration Raman scan to examine two small turbostratic (TS) peaks at ~1880 cm^{-1} and ~2040 cm^{-1}, which are present in turbostratic graphene and absent in ordered graphene. These peaks are also present in FG produced with the arc welder (**Figure 2b**) at a setting of 90, even though the reaction duration is ~20 s, compared to conventional FJH reactions below 5 s. An ordered graphene peak, denoted the M peak, which normally occurs at ~1740 cm^{-1}, is also absent. A transmission electron microscopy (TEM) image of this same FG product (**Figure 2c**) illustrates graphitic ordering, though with an interlayer spacing of 3.47 Å, which is characteristic of turbostratic graphene[1] and is higher than the AB-ordered graphene interlayer spacing of ~3.35 Å. The X-ray diffraction (XRD) pattern of the product (**Figure 2d**) illustrates the high crystallinity of the sample by the narrow (002) peak, and the 3.42 Å interlayer spacing as determined by the position of the (002) peak is well within the 3.4-3.5 Å range seen in metallurgical coke (MC) derived FG.[13]

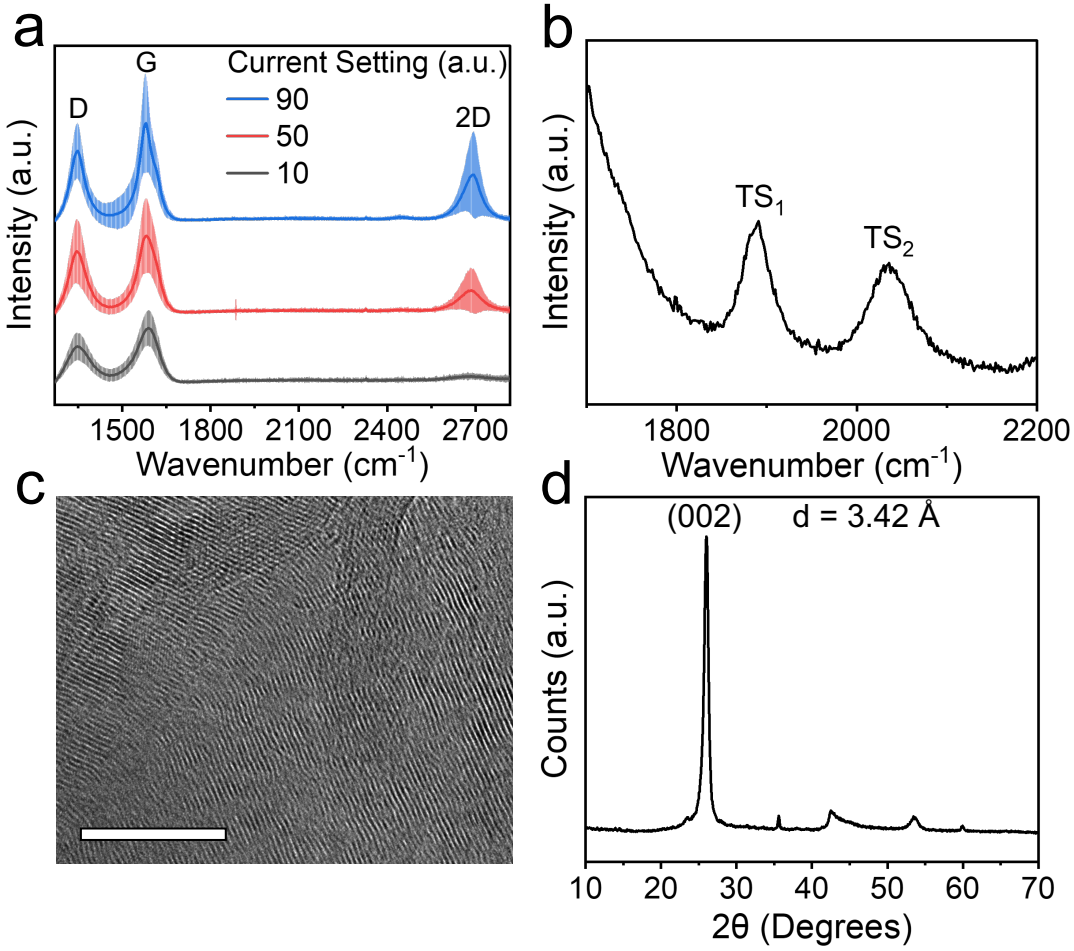

Figure 2. Characterization of FG synthesized using the DEKOPRO arc welder. This FG was synthesized from a 200 mg batch MC at a setting of 90 after a ~20 s flash. a) Average Raman map spectra (n = 200, 532 nm excitation) of 200 mg batches of MC after FJH for ~10 s at different current output settings. The standard deviation of each of these graphs is represented by the shaded area around the line, which is the mean. b) High-resolution Raman spectroscopy illustrates the two turbostratic peaks with the missing M-band, all indicative of turbostratic FG. The intensity ratio of the G peak to the TS_1 peak is ~160. c) TEM image of the FG product. The interlayer spacing measured between the FG layers is 3.47 Å. d) XRD pattern of the FG product. Scale bar, 10 nm (**c**).

2.3 Other Arc Welder Reactions

FJH is also an effective tool for the synthesis of carbon nanotubes (CNTs) from amorphous carbon as well as from waste plastics.[10] This can be achieved through a wet mixing method by which plastic waste is dipped into a water-ethanol solution into which has been dissolved 0.1 wt% ferrocene. This waste plastic product is electrically resistive, so it can be mixed with a conductive additive before it is placed in the quartz tube, such as carbon black or MC, to reduce its resistivity and enable FJH. CNTs begin to form by FJH at as low as ~800 ºC and can coexist with FG in reactions that occur at ~2000 ºC. Temperatures higher than this form a greater portion of FG with lower portions of the CNT product.[10] Accordingly, we flashed waste plastic (high-density polyethylene, HDPE) with ferrocene, mixed with 20 wt% carbon black as the conductive additive, using the same DEKOPRO commercial arc welder, at a 200 mg sample size of this mixture, in a fused quartz tube. The arc welder was turned to a setting of 70 and the mixture was heated for 10 s to produce a mixture of CNTs and FG. **Figure 3a** illustrates the Raman spectra of the product, which consists of successfully converted FG as well as CNTs, as evidenced by the radial breathing mode (RBM) Raman peaks at ~220 cm^{-1} and ~285 cm^{-1}. Scanning electron microscopy characterization of this same product (SEM, **Figure 3b**) shows the CNTs, which exhibit a diameter of ~100 nm, typical of multiwall CNTs formed from this method.[10] This reaction was performed at a comparatively low arc welder setting and thus exhibited some regions of amorphous carbon in addition to FG, demonstrating that CNTs can be made with or without FG (**Figure S5**). Raman spectroscopy analyses of the RBMs of the CNTs using two different Raman excitation wavelengths were performed (**Figure 3c**). Additional SEM and EDAX analysis is shown in **Figure S6**. A simplified mixing technique can also be used with the arc welder, whereby the ferrocene is

mixed directly into the plastic-carbon black mixture, without any wetting or drying steps. This method also produced CNTs, though with a lower yield than with the wet mixing method **(Figures S7-S8)**.

The versatility of FJH reactions also enables the synthesis of heteroatom-doped FG.[22] To achieve this, heteroatom-containing compounds are mixed in with the amorphous carbon reactant. The resulting mixture is then FJH to produce heteroatom-doped FG. A variant of this technique involves flashing the heteroatom compound in the presence of FG to achieve a still higher doping concentration, termed heteroatom-substituted reflash graphene. Motivated by these and by the previous work on destroying harmful per- and polyfluorinated alkyl substances (PFAS),[23,24] we synthesized heteroatom-substituted reflash graphene using the DEKOPRO arc welder to perform an FJH reaction on a 200 mg mixture of perfluorooctane sulfonic acid (PFOS) and MCFG mixed in a 1:4 weight ratio. The resulting product achieved ~9% fluorine substitution, as demonstrated by X-ray photoelectron spectroscopy analysis (XPS, **Figure 3d**). Tube FJH reactions with this DEKOPRO arc welder can be performed in even gram-scale batch sizes, still affording successful graphene conversion (**Figure S9**). This near-constant heating rate also illustrates the thermodynamics of the graphene reaction, since the first temperature maximum at ~5 s arising from the graphene and MC volatiles exotherm is visible (**Fig S9c**).[16] FJH has also been effectively used in the upcycling of glass fiber reinforced plastics (GFRP) to efficiently produce SiC.[11] Using a higher-power arc welder, such as an Amico Electric ARC-200DC, enables upcycling of GFRP into SiC within the quartz tube even up to a 6 g scale reaction (**Figures 3e-3f).**

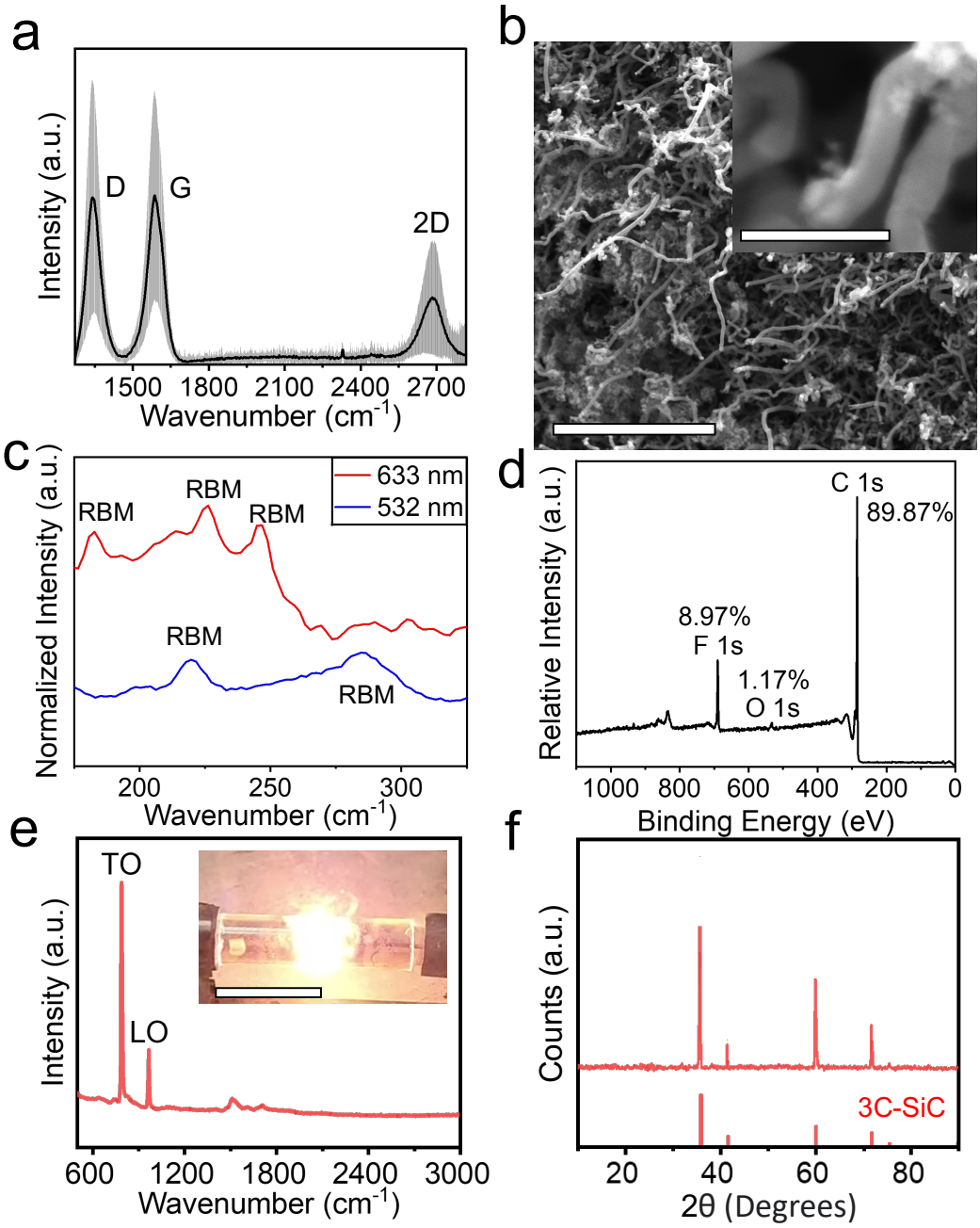

Figure 3. Additional FJH synthesis applications of the arc welder systems to form CNTs, heteroatom-substituted graphene, and SiC. a) Average Raman spectrum (n = 200, 532 nm excitation) of CNTs and FG synthesized from ferrocene and plastic waste. b) SEM image of CNTs from this same product. c) High resolution Raman spectra of the RBMs of the innermost tubes of the multiwall CNTs synthesized, using two different Raman excitation wavelengths. CNT index

assignment is performed in **Figure S10.** d) XPS spectrum of the products of the PFOS-MCFG FJH reaction. Fluorine substitution into the FG lattice is achieved at ~9 at%. e) Raman spectrum of SiC product resulting from FJH of 6 g mixture of GFRP-MC in a 2:1 mass ratio followed by combustion of the FG. The inset image is a photo of this FJH reaction. f) X-ray diffraction pattern of the SiC product of this FJH reaction after a furnace heating step to combust the FG. The spectrum is illustrated above the corresponding powder diffraction file of 2H-SiC. Additional characterization and discussion are in **Figures S11-S12.** Scale bars, 5 μm (**b**); 400 nm (**b**, inset); 4 cm (**e**).

2.4 Other Commercial Systems

The DEKOPRO arc welder offers vastly superior price, temperature controllability, and ease of use compared to conventional FJH electrical systems. However, other heating systems can offer higher power output and still higher temperature controllability than even the DEKOPRO system, all while remaining far more economical and facile than conventional FJH systems (**Figures S13-S14)**. Several alternative systems for FJH were examined and tested, with prices ranging from $125 to $6500 (**Table S1, Figure S15**). These systems each exhibit different voltage, current, and thus power ranges, which also depends by Ohm's Law on the sample resistance (**Figure S16**). To explore the effects of these systems on FG conversion, we synthesized FG, and we recycled electronic waste[8] using both an alternating current (AC) Powerstat variable transformer and a direct current (DC) Zhaoxin programmable power supply (**Figure S17**). In doing so, we successfully demonstrate FJH reactions using both AC and DC power sources. Additional similar electrical and thermal characterization of the outputs of these two systems are included in **Figures S18-S23.**

While the monetary cost per kilowatt output of programmable power supplies is in general higher than that of arc welders, they offer higher controllability, typically in increments of 0.1 A and 0.1 V. In contrast, arc welders do not typically feature voltage controllability and exhibit current controllability of ~1 A. The high controllability of the programmable power supply facilitates thermodynamic analysis of FJH reactions. Though not demonstrated here, programmable power supplies could also be used in a feedback mode with a temperature monitor to provide additional sample temperature stability. **Figure S18** illustrates the FJH conversion of MC into MCFG at constant power, except for a brief spike at the beginning. The results from this experiment illustrate that even with constant power output, the conversion of MC to MCFG experiences two temperature maxima: one from the Joule heating, and one from the 34 kJ mol^{-1} exotherm of the reaction.[16]

We previously reported that the use of an oscillating current, such as a pulse-width modulated DC current, during FJH affords superior FG conversion compared to FG formed from a non-oscillating current.[13,16] Performing a fast Fourier transform on the output current signals of the arc welders **(Figures S24-S28)** reveals that the arc welders output with a duty cycle of multiple different frequencies, including one at ~9.6 kHz. This provides the arc welders with an innate advantage in the FJH synthesis of FG and other 2D materials, compared to conventional flash Joule heaters. Additionally, arc welders can be arranged in series or parallel to increase power output (**Figures S29-S30**). The power source of the arc welder can also be tuned. Rather than connecting to a stationary power outlet, a simple system can be constructed whereby an arc welder can be powered by a portable power system. We thus assembled this system, using a car battery, which was charged

from solar panels, to enable a portable flash Joule heater that operates entirely on solar power **(Figures S31-S32)**, which can be assembled for only $422 **(Table S2)**.

2.5 Arc Heating

Arc welders are specifically designed to facilitate arc heating by automatically raising the DC voltage in its open circuit state until an arc is formed, at which point the voltage decreases. This same technique has been recently repeated with a TDK Lambda GENESYS power supply in order to perform ultrahigh temperature plasma synthesis by creating an arc across layers of carbon felt.[25] This technique is also possible using arc welders, which are typically 1/30 the cost of programmable power supplies of comparable power output, even across carbon paper (**Figure S33**).

Arc melters have been a widely used tool in inorganic synthesis for decades as ultrafast reactors and are thus commonly present in solid-state synthesis laboratories. They are comprised of an arc welder, which provides the heating, connected to an evacuated chamber wherein a user-controlled needle electrode operates as one electrode, and a copper or brass mortar onto which the reactants are placed operates as the other electrode. Motivated by this, we also tested a Lincoln Electric Precision TIG 275 arc welder connected to an arc melter chamber, using a copper mortar and a 2% lanthanated tungsten electrode, to use arc heating to convert MC into MCFG. The metal presence in the electrodes provided sufficient catalyst to form carbyne chains, rapidly identified by a prominent C band, measured by Raman spectroscopy in different samples from ~1770 cm^{-1} to ~1840 cm^{-1} using multiple excitation wavelengths (532 nm, 633 nm, and 785 nm). Though not studied here by TEM, the unique Raman diagnostic signals are definitive fingerprints of their

presence. These carbyne chains are likely bound inside and stabilized by multiwall CNTs on the surface of the MCFG (**Figures S34-S37**).[26,27] This technique had previously only been achieved using higher value, 99.99% graphite rods, and had not previously been reported on a separate feedstock.[26,27]

2.6 Kilogram Scale FG Production

Previous attempts at scaling up FJH reactions have been made by rapidly automating small, gram-scale batches of feedstock to achieve cumulative large-scale synthesis over time, even up to kilogram-scale in hours. These FJH systems tend to involve elaborate automation assemblies.[13] Arc welders provide a facile alternative to scaled and customized FJH system, can be operated rapidly, require minimal training, and are less than 1% of the cost of dedicated FJH systems. A kilogram-scale FG reaction using an Amico Electric ARC-200DC arc welder is shown in **Figure 4**. The reactor consists of this arc welder connected to two graphite rods, placed inside a 13 L, $9.97 clay flowerpot (Home Depot) that is filled with 500 g MC and open to the air (**Figures 4a, S38**). Unlike large Pyrex beakers that cracked under these thermal stresses, the flowerpots remained uncracked. The arc welder cathode (negative) clamp was attached to the end of a 0.2 m long, 16 mm diameter graphite rod ($15.99, Amazon), and the anode (positive) clamp was attached to the end of a 0.2 m long, 8 mm diameter graphite rod ($4.80, Amazon). The pot is placed atop a $52.99 JAYEGT Motorized Rotating Display Stand rotating platform system (22 cm, 250 lbs load rating, wired, Amazon). When the arc welder is turned on, an electric current is permitted to flow across the two graphite electrodes, and rotation of the platform at ~3 rpm automatically stirs the reactor and ensures uniform heating (**Figure 4b**). The FJH electrodes are also moved during the reaction to heat a different radius of sample (**Figures S39, S40**). The long duration of this reaction

permits the exertion of enough energy to convert the entire 500 g of MC to MCFG (**Figures 4c, 4d**). The temperature of the reaction reaches over 3000 ºC (Micro-Epsilon CTRM1H1SF100-C3 pyrometer), while the average sample resistance decreases during conversion (**Figure S41**). Batches can be easily loaded and unloaded into the reaction vessel, and thus two consecutive reactions were performed to achieve 1 kg MCFG in total product after 20 min of heating. This technique was also used to FJH a 900 g batch of waste GFRP and MC, mixed in a 1:2 weight ratio, to produce SiC (**Figures 4e, 4f, S42**) as well as a mixture of 50 g HDPE loaded with 1 wt% ferrocene (we used this higher ferrocene loading in the flowerpot reactor since it was added as a solid) was also mixed with 500 g MC to grow CNTs on the MC (**Figure S43**). FJH reactions become more efficient at large scales, since most of the heat is transferred into the reaction instead of out to the environment (**Figure S41)**.[16] This production method features a higher production rate than other scaled and automated FJH production methods reported in the literature by a factor of up to 220(ref17) and is also more energy efficient, producing graphene with ~60% less energy per product mass (**Figure 4e**).[13,17,28] Simultaneously, this reaction system can be constructed at ~1/160th the cost of even milligram-scale commercially sold FJH systems.[29] Production rate can be further increased by using multiple arc welders simultaneously, in series to increase maximum output voltage or parallel to increase maximum output current, which is up to 30 times more cost-effective than purchasing larger power supplies (**Figure S44**). Flashing with arc welders in series or using a power supply that outputs higher voltage is also an effective way to heat a larger volume at a time (**Figure S45**). Product uniformity could also be improved using additional stirring (**Figure S46**) and electrode configurations (**Figure S47**). Adding a simple automated loading and unloading process could enable continuous production of FG from carbon or waste materials

(**Figure S48**). Finally, flashing MC in this scaled reactor at higher energy per mass will convert the initial turbostratic (disordered) MCFG into ordered FG and graphite[16] (**Figure S49**).

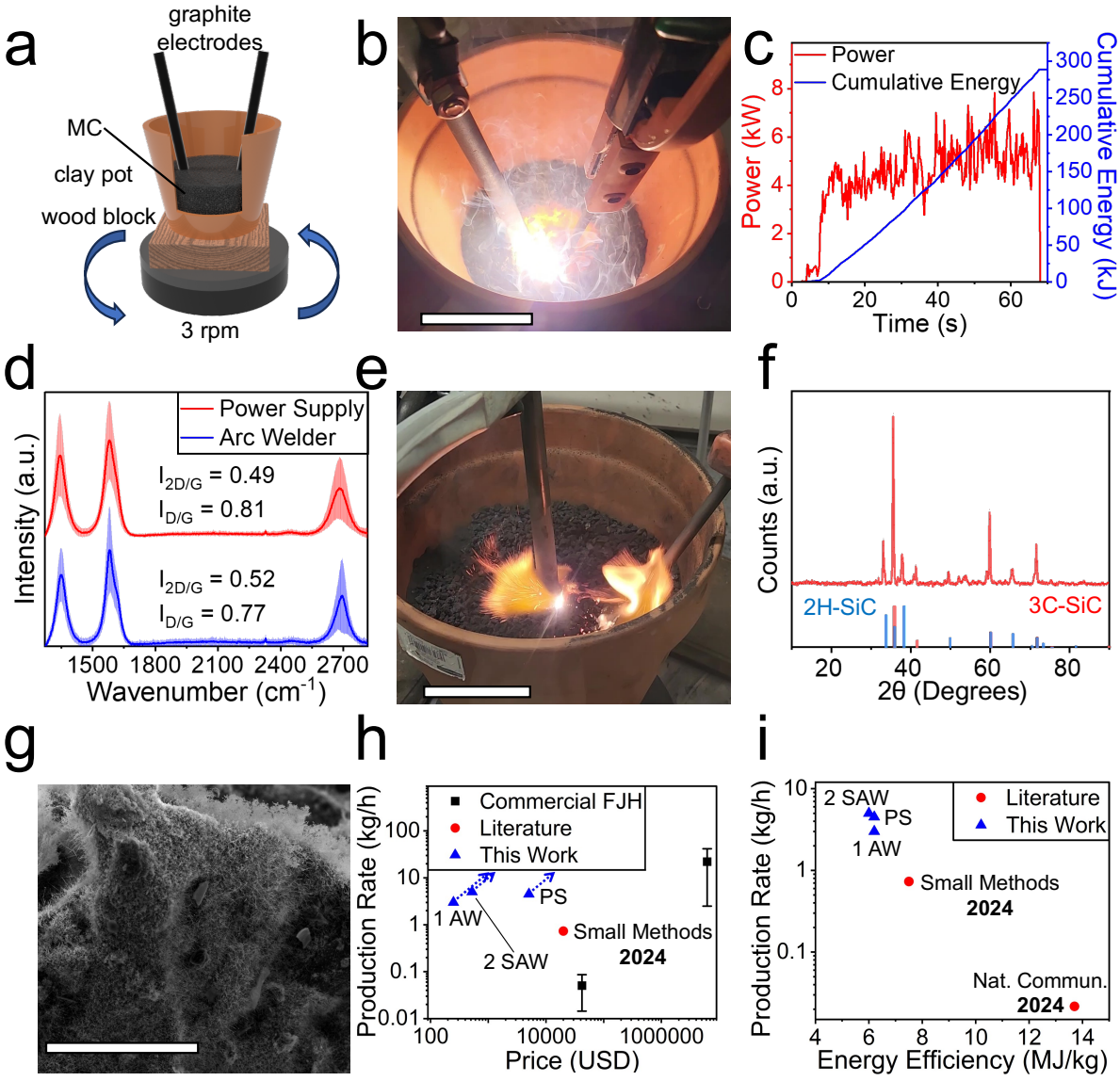

Figure 4. Kilogram scale FJH reaction using the $180 Amico Electric arc welder on MC. a) Schematic image of the clay pot filled with MC. A cross section has been cut out to show the contents. b) Photo of the arc welder in use on ~750 g MC in a clay pot, turning on a rotating platform at ~3 rpm, as shown in the Supplementary Video, reacting for 10 min at 3 kg/h FG

production. c) Power and cumulative energy usage of a ~70 s MC reaction plotted with respect to time. d) Average Raman spectra (n = 200, 532 nm excitation) of the FG product synthesized both using the Amico Electric arc welder and a TDK Lambda GEN 125-80 power supply. The standard deviation of each of these graphs is represented by the shaded area around the line, which is the mean. e) Photo of the arc welder in use on a mixture of ~900 g GFRP and MC, producing SiC at a rate of 430 g/h. f) XRD pattern of SiC produced from the scaled synthesis method after FG removal by furnace treatment. The powder diffraction files of both 2H-SiC and 3C-SiC are illustrated below, demonstrating that both phases of SiC were produced. Additional X-ray photoelectron spectroscopy (XPS), XRD and thermogravimetric analysis (TGA) characterization is exhibited in **Figures S50-S51**. g) SEM image of CNTs on MC produced during a 550 g scaled reactor flash. h) FG production rate plotted as a function of system price comparing using a single Amico Electric arc welder (1 AW), 2 Amico Electric welders in series (2 SAW), and the TDK Lambda power supply (PS) with this scaled reactor compared to commercially available FJH systems from ACS Materials LLC, and a scaled FJH system previously reported by our group.[13] The error bars from the commercial FJH systems illustrate the range of production rates quoted by ACS Materials LLC for these FJH models. The cost of the clay pot, the turning platform, the electrodes, and all arc welder parts are included in these values. The blue dotted line illustrates the cost and production rate of duplicating each system. For example, having 2 AWs and 2 flowerpot reactor systems running concurrently would cost $520 and produce 6 kg/h MCFG, which is superior cost efficiency relative to using a single reactor system with 2 SAW at $530 and 5 kg/h. i) FG production rate plotted as a function of energy efficiency comparing using 1 AW, 2 SAW the PS with this scaled reactor, to others reported in the literature.[13, 17] Scale bars, 10 cm (**b**); 10 cm (**e**); 200 μm (**g**).

2.6 Inorganic Synthesis Reactor

FJH has also been used in the synthesis of 22 inorganic compounds, primarily transition metal dichalcogenides (TMDs) and p-block metal dichalcogenides (PMDs), through a method called flash-within-flash synthesis.[2] By this technique, inorganic reactants are filled inside an inner quartz tube, which is then surrounded by a feedstock such as MC, before being inserted into another quartz outer tube and closed at the end with electrodes, usually made of graphite. The outer tube undergoes a conventional FJH reaction in which electrical current passes through the MC, heating it. This hot MC then passes heat to the inner tube and its inorganic feedstock contents through thermal conduction. Current does not need to flow through the inorganic feedstock contents of the inner tube in this process, and thus this inorganic feedstock is not restricted to any electrical resistivity boundaries typical of conventional FJH. Inspired by this technique, we performed a flash-within-flash reaction using the scaled reactor technique (**Figure 5**) and prepared 9 quartz tubes: 5 loaded with 0.4 g $SnCl_2 \cdot 2H_2O$ plus 1.0 g Se powder and 4 loaded with 0.4 g $SnCl_2 \cdot 2H_2O$ and 1.0 g S powder for a total of 12.6 g of feedstock. These tubes were embedded in the MC until completely covered in a nonagonal pattern around the center electrode (**Figures 5a, 5b**). The mixture was then subjected to FJH using an analogous technique to that shown in **Figure 4** in which the arc welder electrodes moved in a circular motion around the quartz tubes, FJH the MC and hence transferring this heat through thermal conduction to the tubes. The result of this 1-min synthesis was 5 tubes each containing ~0.2 g SnS_2 and 4 tubes each containing ~0.15 g $SnSe_2$ products (**Figures 5c-5i, S52**), amounting to a PMD production rate of 100 g h^{-1}. The versatility of this scaled FJH reactor distinguishes it as a viable inorganic reactor by which several different inorganic products can be simultaneously synthesized. Furthermore, the value of the FG byproduct

produced around these tubes offsets the cost of these reactions such that the inorganic products are synthesized at a negative net cost.

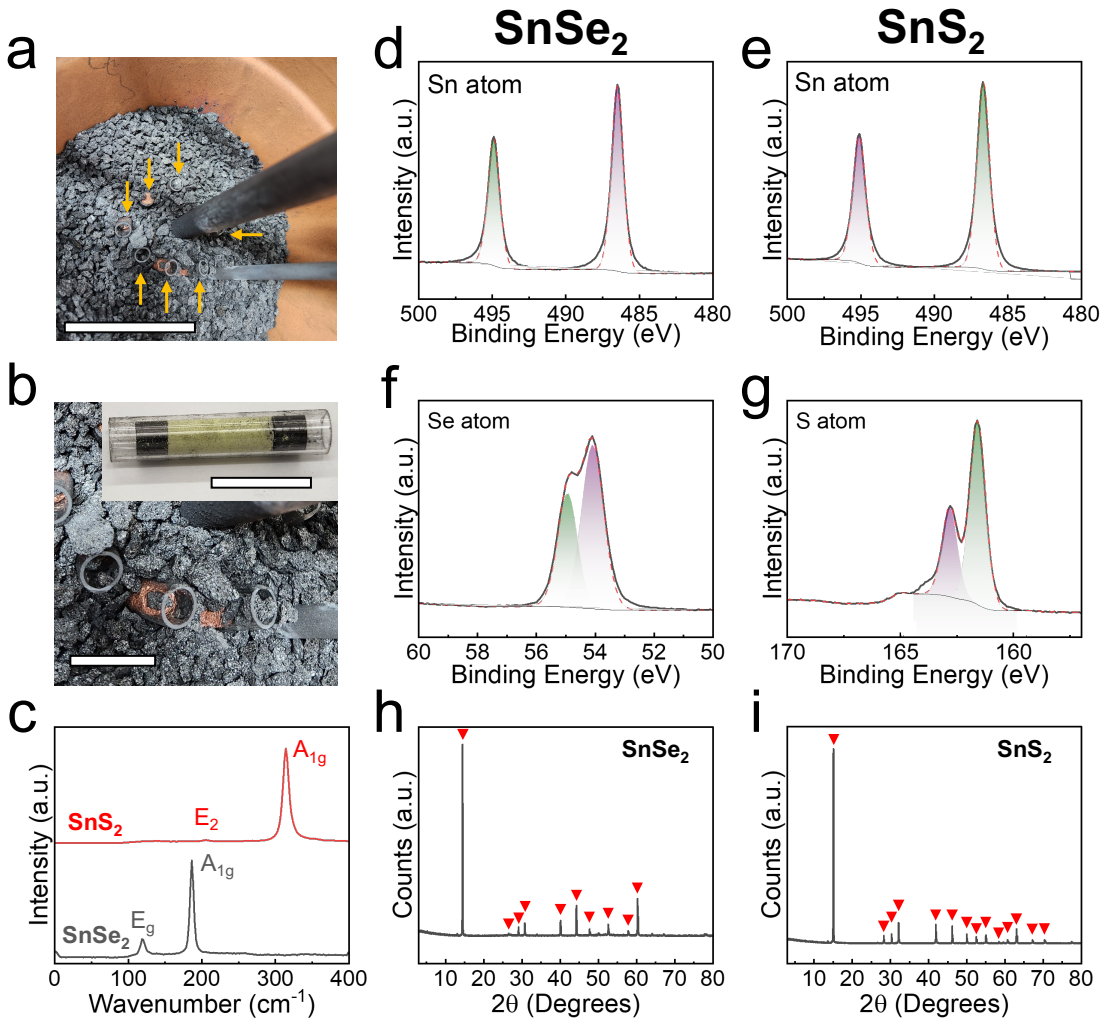

Figure 5. Simultaneous flash-within-flash reactions performed using the Amico Electric welder. a) Image of the 9 tubes filled with the inorganic reactant feedstock embedded in MC inside the clay flowerpot. Yellow arrows point to the tubes that are visible in the photo. b) Zoomed-in image of the tubes inside the flowerpot. The inset photo shows a single tube loaded with 0.4 g $SnCl_2 \cdot 2H_2O$ and 1.0 g S powder. c) Raman spectra of SnS_2 and $SnSe_2$. d) XPS spectrum illustrating Sn in the $SnSe_2$ product. e) XPS spectrum illustrating Sn in SnS_2 product. f) XPS spectrum

illustrating Se in the $SnSe_2$ product. g) XPS spectrum illustrating S in SnS_2 product. h) XRD pattern of $SnSe_2$. i) XRD pattern of SnS_2. Scale bars, 10 cm (**a**); 2 cm (**b**; **b**, inset), 10 nm (**g**).

3 Conclusions

Commercial power supplies, especially arc welders, provide a far less expensive, more accessible, standardized, more scalable, and more temperature controllable alternative to conventional FJH systems. This facilitates FJH synthesis, especially in reactions requiring greater temperature controllability and those that require sustained heating over longer durations of seconds or minutes. Innate pulse width-modulation in the arc systems reduces the energy requirement to synthesize high-quality FG relative to systems using unmodulated direct current. Pairing these systems with new reaction geometries and systems also enables facile larger scale synthesis by FJH to kilogram scale (**Figure S53**), even in the open air since outgassing prevents oxidative degradation.

4 Experimental Section

Materials

Metallurgical coke was obtained from SunCoke in chunks ~10 cm in diameter. These chunks were then ground and sieved. Additional characterization of this raw material has been previously reported.[13]

GFRP for the scaled reactor was obtained in the form of Garolite G-10 sheets purchased from Amazon. These sheets were then cut and ground by a hammer mill into a fine powder of 300 g in mass. This powder was then mixed with small grain (0.05-0.15 mm) MC in a 2:1 ratio to make 900 g of GFRP-MC mixture.

For the scaled flash within flash synthesis of p-block metal dichalcogenides, $SnCl_2 \cdot 2H_2O$ powder (CAS# 10025-69-1) was obtained from Alpha Aesar. Sulfur powder (CAS# 7704-34-9) was obtained from Millipore Sigma. Se powder (CAS# 7782-49-2) was obtained from Millipore Sigma.

For the synthesis of CNTs in the small tube reactions, $FeCl_3$ (CAS# 7705-08-0) was obtained from Millipore Sigma. Carbon black BP2000 was obtained from Cabot. High-density polyethylene was obtained from Millipore Sigma. For the scaled reactor, ferrocene ($Fe(C_5H_5)_2$ CAS# 102-54-5) was obtained from Millipore Sigma.

Scaled FG Reaction

750 g large MC grains (1.7-3 mm) were poured into a terra cotta flowerpot. The pot was obtained from The Home Depot (Store SKU # 208337) for $9.97 and had a height of 21.0 cm, a top diameter of 25 cm, a bottom diameter of 14.6 cm, a total volume of 13 L, and a mass of 2.2 kg. The arc welder cathode (negative) clamp was attached to the end of a 0.2 m long, 16 mm diameter graphite rod ($15.99, Amazon) and the anode (positive) clamp was attached to the end of a 0.2 m long, 8 mm diameter graphite rod ($4.80, Amazon). Each arc welder clamp was itself held above the pot by a chemical clamp mounted on a laboratory clamp stand. These rods were then embedded ~3 cm deep into the MC, with the large graphite rod (anode, positive) inserted laterally in the center of the pot and the small graphite rode (cathode, negative) inserted laterally ~6 cm away from the large rod (**Figure S38)**. These arc welder electrodes were plugged in to an Amico Electric ARC-200 DC arc welder purchased from Amico Electric for $179.00, which itself was plugged in to a 208 V, single phase, AC outlet. The clay pot was often mounted onto a wooden block (rectangular prism

shape, 3 cm height, 8 cm side length) to add a layer of thermal and electrical insulation below the pot and to cover the hole at the bottom of the flowerpot. The pot and wood block were then mounted onto a JAYEGT Motorized Rotating Display Stand (22 cm, 250 lbs load rating, wired) purchased from Amazon for $52.99. The rotating platform was then turned on and began spinning at ~3 rpm. Since the pot was placed on top of the turning stand, but the electrodes were held independently, the pot and the MC mixture within rotated relative to the electrodes in order to permit more uniform heating (**Figure S38**). The heating procedure is illustrated in **Figure S40**. To begin the FJH reaction, the arc welder dials (arc force and output current dials) were then turned maximum output such that the screen of the arc welder displayed an output value of 200. The reaction proceeded under this orientation for 5 min, during which the lateral center of the sample, near the surface, was heated and converted to MCFG (**Figure S39a**). The center electrode (anode) was then moved laterally to the outer radius of the pot such that it was still ~6 cm from the cathode, but now ~8 cm from the center of the pot (**Figure S39b**). This movement of the electrode was achieved by laterally moving the laboratory clamp stand holding the electrode. Heating continued in this orientation for 2.5 min, during which the outer lateral radius of MC near the surface was heated (**Figure S40**, step 3). After this, a 3rd electrode orientation was implemented by first moving the outer electrode to the lateral center of the pot by again moving the laboratory clamp stand. Then, both electrodes were pushed deeper into the pot to a depth of ~6 cm into the MC (**Figure S40**, step 4). The reaction then continued for another 2.5 min. Of the 750 g of MC in the pot, the top-center 500 g MC was removed, and the bottom 250 g MC was left behind (**Figure S40**, step 5). Only this top 500 g was characterized (**Figure 5d**) and counted toward the MCFG production rate. 250 g MC was left behind since this MC has low (~10%) conversion to MCFG, and this remaining MC adds a layer of thermal protection to the flowerpot, allowing the flowerpot to

survive multiple FJH cycles. After the 500 g of MCFG are removed, an additional 500 g of MC are added to the flowerpot, bringing the total again to 750 g in preparation for another reaction. This FJH procedure was then repeated once more to recover an additional 500 g of MCFG product to accumulate a total of 1 kg MCFG. This single arc welder method thus uses three separate heating steps: the first heating step with a 5 min duration, the second heating step with a 2.5 min duration, and the third heating step with a 2.5 min duration, for a total heating duration of 10 min for 500 g of MCFG production. Thus, a 500 g/10 min (3 kg/h) production rate is counted.

This MCFG production procedure was also analogously performed with two Amico Electric ARC200-DC arc welders in series (**Figures S29a, S30a**), assisted using two power diodes, instead of only one arc welder in order to increase the production rate. When two arc welders in series are used, then the process proceeds identically, except that the inter-electrode distance is ~8 cm, instead of the 6 cm used for a single arc welder, and the first heating step had a 3 min duration, the second a 1.5 min duration, and the third a 1.5 min duration, for a total heating duration of 6 min for 500 g of MCFG production. Thus, a 500 g/6 min (5 kg/h) production rate is counted. The two arc welders were also only turned onto a screen-displayed current setting of 150 for FJH when connected in series instead of the maximum (200) setting when a single arc welder was used.

This procedure was also analogously performed using the 10 kW TDK Lambda GENESYS GEN 125-80-3P208 programmable power supply. The MCFG production procedure for FJH with the power supply is identical to that for a single arc welder, except that the inter-electrode inter-electrode distance is ~8 cm, instead of the 6 cm used for a single arc welder, and the first heating step had a 3 min duration, the second a 1.7 min duration, and the third a 2 min duration. This total

heating duration (6.7 min) is considered for 500 g of MCFG production, for a production rate of 500 g/6.7 min (4.5 kg/h). The power supply was turned to its maximum setting (125 V, 80 A) during this FJH reaction.

Scaled SiC Reaction

A schematic illustration of the SiC reactor is shown in **Figure S42**. Prior to flashing in the scaled reactor, the 300 g GFRP powder was hand-mixed with 600 g of MC powder (0.05-0.15 mm) to make a 1:2 GFRP-MC mixture (further described in materials section). 500 g of large MC grains (1.7-3 mm) were used to fill the bottom of the 13 L terra cotta flowerpot to act as thermal insulation. A square Garolite G-10 GFRP plate was purchased from Amazon for $14.95 (257.5 mm side length, 2.0 mm thickness, 702401461076) was cut with a bandsaw to a circular shape (~18 cm diameter) to fit inside the pot. This GFRP was then placed and rested upon this large grain MC layer to prevent fine grains of GFRP-MC mixture from falling to the bottom of the pot. 300 g large MC grains (1.7-3 mm) were then used to fill the volume in the pot above the plate. The 900 g of 1:2 GFRP-MC powder mixture was then poured above large grain MC layer. The arc welder cathode (negative) clamp was attached to a 0.2 m long, 16 mm diameter graphite rod and the anode (positive) clamp was attached to a 0.2 m long, 8 mm diameter graphite rod. Each arc welder clamp was itself held above the pot by a chemical clamp mounted on a laboratory clamp stand. These rods were then embedded ~3 cm deep into the GFRP-MC mixture, with the large graphite rod (anode, positive) inserted laterally in the center of the pot and the small graphite rode (cathode, negative) inserted laterally ~6 cm away from the large rod (**Figure S38)**. These arc welder electrodes were plugged into two Amico Electric ARC-200 DC arc welders connected in a series configuration as illustrated in **Figures S29a, S30a**. Each of these arc welders were themselves

plugged into a 208 V, single phase, AC outlet. The use of two arc welders in series rather than only one arc welder increases the production rate and the voltage of the arc welder series system, allowing this higher resistance GFRP-MC sample to more easily be heated, as described in **Figure S45**. The clay pot was mounted onto a wooden block (rectangular prism shape, 3 cm height, 8 cm side length) to add a layer of thermal and electrical insulation below the pot. The pot and wood block were then mounted onto a JAYEGT Motorized Rotating Display Stand. The rotating platform was then turned on and began spinning at ~3 rpm. The heating procedure is illustrated in **Figure S40**. To begin the FJH reaction, the arc force dials on both systems were turned to their maximum setting, and the current dials output on both systems were adjusted so that a value of 40 was displayed on the screens of each arc welder. The reaction proceeded with these settings for 1 min in order to pretreat the GFRP-MC feedstock, making it more conductive (**Figure S40**, step 1). For the second step, the current output dials of both arc welders were then each increased so that a value of 80 was displayed on the screens of each arc welder. Simultaneously, the rotating platform was turned on and began spinning at ~3 rpm. The reaction proceeded under this configuration for 5 min, during which the lateral center of the sample, near the surface, was heated and converted to SiC (**Figure S39a**). The reaction was paused for ~30 s by turning off the arc welders and the turning platform, and the electrodes were manually operated to push some of the GFRP-MC powder mixture back to the radial center of the reactor. The center electrode (anode) was then moved laterally to the outer radius of the pot such that it was still ~6 cm from the cathode, but now ~8 cm from the center of the pot (**Figure S39b**). This movement of the electrode was achieved by laterally moving the laboratory clamp stand holding the electrode. Heating continued in this orientation for 5 min at the previous arc welder current output settings (80 a.u.) and turning platform rotation rate (~3 rpm), during which the outer lateral radius of GFRP-MC near the surface

was heated (**Figure S40**, step 3). The reaction was paused again for ~30 s by turning off the arc welders and the rotating platform, and the graphite electrodes were again manually used to stir the unreacted portion of the GFRP-MC powder mixture to the radial center of the reactor. The initial electrode configuration was restored (**Figure S40**, step 2), the arc welders were turned back on to their previous current output setting (80 a.u.), and the turning platform was turned on again. Heating resumed for another 3 min. Finally, the arc welders and the rotating platform were turned off. Thus, this single arc welder method thus uses four separate heating steps and two pauses during which manual mixing is performed: the first preheating step with a 1 min duration, the second heating step with a 5 min duration, the first pause with a ~40 s duration, the third heating step with a 5 min duration, the second pause with a ~40 s duration, and the fourth heating step with a 3 min duration, for a total process duration of 15.3 min. After this process, the centermost ~110 g of product is removed for characterization and was identified as SiC. The rest of the feedstock was less well-reacted and was thus left behind. Thus, a 110 g/15.3 min SiC production rate (0.43 kg/h) is counted.

Quartz Tube Synthesis of CNTs

For the high-yield method, a surface-wetting method was used to load metal catalyst onto HDPE.[10] HDPE was purchased from Polywize and ground using a 1400 rpm, 110 V micro plant grinder. A solution of 80%/20% v/v mixture of water and ethanol was prepared, and $FeCl_3$ at a concentration of 0.1 g mL^{-1} was dissolved in the solution. 5 g of <0.1 mm grain size HDPE was submerged in 15 mL solution and sonicated for 15 min. Solvent was evaporated for 30 min with a rotary evaporator and then placed under a vacuum for 3 h. Afterwards, the sample was dried at room temperature for 18 h. 80 wt% catalyst-loaded HDPE was ground with 20 wt% amorphous carbon

black (Cabot) using a mortar and pestle. 0.20 g of the HDPE and carbon black homogenous mixture was loaded into a quartz tube with an internal diameter of 8 mm. A copper wool plug and a graphite electrode were used to compress the sample.

Scaled CNT-MCFG Reactor

A schematic illustration of the scaled CNT-MCFG reactor is shown in **Figure S43**. 50 HDPE was mixed with 0.5 wt% ferrocene and compressed into pellets ~1 cm in diameter. These pellets were then mixed with 500 g large grain MC (1.7-3 mm). 500 g of large MC grains (1.7-3 mm) were used to fill the bottom of the 13 L terra cotta flowerpot to act as thermal insulation. 500 g mixture of MC and ferrocene-loaded HDPE was mixed and filled the top of the container, resting upon the 500 g large MC grains. The arc welder cathode (negative) clamp was attached to a 0.2 m long, 16 mm diameter graphite rod and the anode (positive) clamp was attached to a 0.2 m long, 8 mm diameter graphite rod. These rods were then embedded ~3 cm deep into the HDPE-MC mixture, and ~4 cm apart. Each arc welder clamp was itself held above the pot by a chemical clamp mounted on a laboratory clamp stand. These rods were then embedded ~3 cm deep into the HDPE-MC mixture, with the large graphite rod (anode, positive) inserted laterally in the center of the pot and the small graphite rode (cathode, negative) inserted laterally ~4 cm away from the large rod (**Figure S38)**. These arc welder electrodes were plugged into two Amico Electric ARC-200 DC arc welders connected in a series configuration as illustrated in **Figure S29a, S30a**. Each of these arc welders were themselves plugged into a 208 V, single phase, AC outlet. The use of two arc welders in series rather than only one arc welder increases the production rate and the voltage of the arc welder series system, allowing this higher resistance HDPE-MC sample to more easily be heated, as described in **Figure S45**. The clay pot was mounted onto a wooden block (rectangular

prism shape, 3 cm height, 8 cm side length) to add a layer of thermal and electrical insulation below the pot. The pot and wood block were then mounted onto a JAYEGT Motorized Rotating Display Stand. The rotating platform was then turned on and began spinning at ~3 rpm. Since the pot was placed on top of the turning stand, but the electrodes were held independently, the pot and the feedstock mixture within rotated relative to the electrodes in order to permit more uniform heating (**Figure S38**). The heating procedure is illustrated in **Figure S40**. To begin the FJH reaction, the arc force dials on both systems were turned to their maximum setting, and the current dials output on both systems were adjusted so that a current output value of 60 was displayed on the screens of each arc welder. This configuration and system setting was maintained during 2.5 min of pretreatment flashing, as illustrated in step 1 of **Figure S40**. This pretreatment step made the feedstock more conductive to allow a higher current to flow through the sample in subsequent heating steps. For the second heating step, the current output of both arc welders was then adjusted so that a current output of 120 a.u. was achieved, as read from the screens of the arc welders, and the rotating platform was turned on at ~3 rpm. This second heating configuration was maintained for 2.5 min. For the third heating step, the center electrode (anode) was then moved laterally to the outer radius of the pot such that it was still ~4 cm from the cathode, but now ~6 cm from the center of the pot (**Figure S39b**). This movement of the electrode was achieved by laterally moving the laboratory clamp stand holding the electrode. The reaction was allowed to proceed for another 2.5 min in this configuration. during which the outer lateral radius of HDPE-MC near the surface was heated (**Figure S40**, step 3). After this, a third electrode orientation was implemented for a fourth heating step by first moving the anode to the lateral center of the pot by again moving the laboratory clamp stand. The reaction was then continued for another 2.5 min. Thus, the reaction consisted of four heating steps: one pretreatment heating step for 1 min, a second heating step for

2.5 min, a third heating step for 2.5 min, and a fourth heating step for 2.5 min for a total reaction time of 9.5 min. 400 g of the top-center-most feedstock was now obtained as CNT-MCFG product, leaving behind 150 g of poorly reacted HDPE-MC feedstock at the bottom and sides of the container and the initial layer of 500 g MC. Only this 400 g of CNT-MCFG product was considered in the production rate calculation. Hence, a CNT-MCFG production rate of 400 g/9.5 min (2.5 kg/h) was achieved.

Scaled PMD Synthesis

The synthesis of the PMD SnS_2 and $SnSe_2$ was achieved by combining the previously reported flash-within-flash synthesis technique[2] with the scaled reactor, as illustrated in **Figure 5a**. To achieve this synthesis, 500 g large MC grains (1.7-3 mm) were poured into the 13 L terra cotta flowerpot. The arc welder cathode (negative) clamp was attached to the end of a 0.2 m long, 16 mm diameter graphite rod, and the anode (positive) clamp was attached to the end of a 0.2 m long, 8 mm diameter graphite rod. Each arc welder clamp was held above the pot by a chemical clamp mounted on a laboratory clamp stand. These rods were then embedded ~3 cm deep into the MC, with the large graphite rod (anode, positive) inserted laterally in the center of the pot and the small graphite rode (cathode, negative) inserted laterally ~6 cm away from the large rod (**Figure S38)**. These arc welder electrodes were plugged into an Amico Electric ARC-200 DC arc welder, which itself was plugged into a 208 V, single-phase, AC outlet. The clay pot was mounted onto a wooden block (rectangular prism shape, 3 cm height, 8 cm side length) to add a layer of thermal and electrical insulation below the pot. The pot and wood block were then mounted onto a JAYEGT Motorized Rotating Display Stand. Nine fused quartz tubes (4 cm length, 8 mm inner diameter, 12 mm outer diameter) were prepared with the PMD feedstock in the following way: 4 were each

filled with a mixture of 0.4 g $SnCl_2 \cdot 2H_2O$ powder and 1.0 g S powder, and 5 were filled each with a mixture 0.4 g $SnCl_2 \cdot 2H_2O$ powder and 1.0 g Se powder. Each tube was then capped on each end with a tight-fitting graphite cap (cylinder shape, 8 mm diameter, ~6 mm length). These nine quartz tubes were placed evenly spaced in a nonagonal pattern around the center electrode, ~3 cm from the center electrode. Each tube was oriented vertically and embedded 5 cm into the MC so that the tubes were completely covered by the MC. The rotating platform was then turned on and began spinning at ~3 rpm. Since the pot was placed on top of the turning stand, but the electrodes were held independently, the pot and the MC mixture within rotated relative to the electrodes in order to permit more uniform heating (**Figure S38**). To begin the FJH reaction, the arc welder dials (arc force and output current dials) were then turned to maximum output such that the screen of the arc welder displayed an output value of 200. The reaction proceeded for 1 min before the arc welder and the rotating platform were turned off. The 9 quartz tubes were recovered, and an average of 0.2 g of SnS_2 was recovered from the five tubes with Se, and 0.15 g $SnSe_2$ was recovered from the four tubes with S, for a total yield of 1.6 g PMD product. The production rate of 1.6 g/1 min (0.1 kg/h) was thus counted.

Arc Melter

The arc melting process occurs within a custom-designed arc-melter comprising a vacuum chamber surrounded by a cylindrical glass shield, a water-cooled copper crucible featuring grooves for sample placement, and a tungsten electrode tip (2% lanthanated). To initiate an arc, a potential difference is established between the tungsten tip and the samples on the crucible by applying an adjustable DC current (60 – 75 Amps). Simultaneously, a piece of Zr with high oxygen affinity is introduced into the chamber to capture any trace oxygen present. The chamber is evacuated to a

base pressure of 30 mTorr to remove air, after which it is filled with argon gas to facilitate arc formation. The tungsten electrode is then brought closer to the Zr piece to melt it and absorb any residual oxygen. The samples are positioned in separate grooves and are heated by bringing the tungsten tip into contact with them, applying DC current.

Analysis

Raman Spectroscopy Analysis

Raman spectra were collected using a Renishaw inVia microscope outfitted with a 50 mW, 532 nm laser and a 50x objective lens. Except where explicitly stated, all Raman spectra were collected as follows and as previously reported:[13, 19] 2 Raman spectra were measured on each of 100 points across a square 1 mm^2 grid on the sample using a map scan with LiveTrack focusing software enabled. The average Raman spectra shown for each sample is the average of these 200 spectra. The $I_{2D/G}$ and $I_{D/G}$ ratios and their standard deviations are calculated from these 200 spectra per sample as well using a custom Python program as previously described. Graphene yield is a metric that describes the amount of product that has been converted to graphene as a portion of the total product. For the 200 spectra of each sample, a custom Python program first determines the number of these spectra that have a discernible G peak. Among these spectra, the program counts the portion of which that has a $I_{2D/G}$ peak ratio of at least 0.3. This portion is equal to the graphene yield. A spectrum without a discernible G peak in a carbon sample most often results from the Raman laser being insufficiently focused.

Carbon nanotube RBMs were scanned using 10% laser power, for 100 accumulations, at 100 s per accumulation. This data was then smoothened with the OriginLab graphing software using the

Savitzky-Golay method with a 2nd order polynomial. These RBM peak positions identified correspond to the RBMs of the innermost CNTs in the multiwall CNTs synthesized. Relative to the Raman peak positions of the RBMs of single wall CNTs, the innermost CNTs of multiwall CNTs exhibit a blueshift in the Raman signal that is dependent on the innermost CNT diameter,[30] by up to 7% for 1.7 nm diameter tubes.[31] Thus, this blueshift was considered in the assignment by Raman spectroscopy analysis of RBMs to their respective CNT indices. This assignment was then performed by comparing our measured Raman excitation energy and RBM wavenumber values to previously reported values.[32, 33] RBMs can still be excited by a Raman laser off resonance by as much as 0.2 eV.[34]

Transmission Electron Microscopy Analysis

Transmission electron microscopy (TEM) images were collected using FEI Titan Themis operating at 300 keV with the convergence angle of 25 mrad. The aliquot of sample (5 mg of sample/1 mL ethanol) was prepared and was sonicated for 1 h to ensure homogeneous dispersion. The resultant aliquot was drop casted on Cu/lacey carbon TEM grid (Ted Pella). The resultant grid was dried at 80 °C with overnight vacuum drying.

Scanning Electron Microscopy Analysis

Scanning electron microscope images of the arc melter products were taken using an FEI Helios SEM system. All other SEM images were obtained using an FEI Quanta 400 ESEM FEG.

X-ray Diffraction Analysis

X-ray diffractometry scans were performed using a Rigaku Smartlab II using zero background sample holders, a 40 kV, 30 mA X-Ray source, and a Cu K-β filter.

X-ray Photoelectron Spectroscopy Analysis

XPS analysis was performed using a PHI Quantera XPS.

Acknowledgements

The funding of the research was provided by the Air Force Office of Scientific Research (FA9550-22-1-0526, J.M.T.), the U.S. Army Corps of Engineers, ERDC (W912HZ-21-2-0050 and W912HZ-24-2-0027, J.M.T.) and the Welch Foundation (C-2065-20210327, Y.H.), and Rice Academy Fellowship (Y.C.). The characterization equipment used in this project is partly from the Shared Equipment Authority (SEA) at Rice University. We also thank Onur Tosun and Emilia Morosan for their help accessing and using the arc melter system.

Conflicts of Interest

Companies have licensed the FJH approach from Rice University. J.M.T. is a stockholder in those companies, but not an employee, officer, or director. Potential conflicts of interest are mitigated through regular disclosures to and compliance with Rice University's Office of Sponsored Programs and Research Compliance. The other authors declare no conflicts.

References

1 D. X. Luong, K. V. Bets, W. A. Algozeeb, M. G. Stanford, C. Kittrell, W. Chen, R. V. Salvatierra, M. Ren, E. A. McHugh, P. A. Advincula, Z. Wang, M. Bhatt, H. Guo, V. Mancevski, R. Shahsavari, B. I. Yakobson, J. M. Tour, *Nature* 2020, **577**, 647.

2 C. H. Choi, J. Shin, L. Eddy, V. Granja, K. Wyss, B. Damasceno, H. Gao, G. Gao, Y. Zhao, C. F. Higgs, Y. Han, J. M. Tour, *ChemRxiv* 2023, DOI: 10.26434/chemrxiv-2023-h2nph

3 Q. Dong, M. Hong, J. Gao, T. Li, M. Cui, S. Li, H. Qiao, A. H. Brozena, Y. Yao, X. Wang, G. Chen, J. Luo, L. Hu, *Small* 2022, **18**, 2104761.

4 M. G. Stanford, K. V. Bets, D. X. Luong, P. A. Advincula, W. Chen, J. T. Li, Z. Wang, E. A. McHugh, W. A. Algozeeb, B. I. Yakobson, J. M. Tour, *ACS Nano* 2020, **14**, 13691.

5 C. Wang, W. Ping, Q. Bai, H. Cui, R. Hensleigh, R. Wang, A. H. Brozena, Z. Xu, J. Dai, Y. Pei, C. Zheng, G. Pastel, J. Gao, X. Wang, H. Wang, J.-C. Zhao, B. Yang, X. Zheng, J. Luo, Y. Mo, B. Dunn, L. Hu, *Science* 2020, **368**, 521.

6 G. Chen, Y. Wang, X. Wang, Y. Zhao, Q. Dong, L. Hao, M. Hong, M. Guo, H. Qiao, W. Xiong, L. Hu, *ACS Mater. Lett.* 2022, **4**, 480.

7 P. A. Advincula, D. X. Luong, W. Chen, S. Raghuraman, R. Shahsavari, J. M. Tour, *Carbon* 2021, **178**, 649.

8 B. Deng, D. X. Luong, Z. Wang, C. Kittrell, E. A. McHugh, J. M. Tour, *Nat. Commun.* 2021, **12**, 5794.

9 W. Chen, J. Chen, K. V. Bets, R. V. Salvatierra, K. M. Wyss, G. Gao, C. H. Choi, B. Deng, X. Wang, J. T. Li, C. Kittrell, N. La, L. Eddy, P. Scotland, Y. Cheng, S. Xu, B. Li, M. B. Tomson, Y. Han, B. I. Yakobson, J. M. Tour, *Sci. Adv.* 2023, **9**, eadh5131.

10 K. M. Wyss, J. T. Li, P. A. Advincula, K. V. Bets, W. Chen, L. Eddy, K. J. Silva, J. L. Beckham, J. Chen, W. Meng, B. Deng, S. Nagarajaiah, B. I. Yakobson, J. M. Tour, *Adv. Mater.* 2023, **35**, 2209621.

11 Y. Cheng, J. Chen, B. Deng, W. Chen, K. J. Silva, L. Eddy, G. Wu, Y. Chen, B. Li, C. Kittrell, S. Xu, T. Si, A. A. Marti, B. I. Yakobson, Y. Zhao, J. M. Tour, *Nat. Sustain.* 2024, **7**, 452–462

12 B. Deng, R. A. Carter, Y. Cheng, Y. Liu, L. Eddy, K. M. Wyss, M. G. Ucak-Astarlioglu, D. X. Luong, X. Gao, K. JeBailey, C. Kittrell, S. Xu, D. Jana, M. A. Torres, J. Braam, J. M. Tour, *Nat. Commun.* 2023, **14**, 6371.

13 L. J. Eddy, D. X. Luong, J. L. Beckham, K. M. Wyss, T. Cooksey, P. Scotland, C. H. Choi, W. Chen, P. Advincula, Z. Zhang, V. Macevski, J. M. Tour, *Small Methods* 2023, **8**, 2301144.

14 S. Dong, Y. Song, K. Ye, J. Yan, G. Wang, K. Zhu, D. Cao, *EcoMat* 2022, **4**.

15 K. M. Wyss, W. Chen, J. L. Beckham, P. E. Savas, J. M. Tour, *ACS Nano* 2022, **16**, 7804.

16 L. Eddy, S. Xu, C. Liu, P. Scotland, W. Chen, J. L. Beckham, B. Damasceno, C. H. Choi, K. J. Silva, A. Lathem, Y. Han, X. Zhang, Y. Zhao, J. M. Tour, *J. Am. Chem. Soc.* 2024, **146**, 16010.

17 X. Zhu, L. Lin, M. Pang, C. Jia, L. Xia, G. Shi, S. Zhang, Y. Lu, L. Sun, F. Yu, J. Gao, Z. He, X. Wu, A. Li, L. Wang, M. Wang, K. Cao, W. Fu, H. Chen, G. Li, J. Zhang, Y. Wang, Y. Yang, Y.-G. Zhu, *Nat. Commun.* 2024, **15**.

18 K. Sattari, L. Eddy, J. L. Beckham, K. M. Wyss, R. Byfield, L. Qian, J. M. Tour, J. Lin, *Digit. Discov.* 2023, **2**, 1209.

19 J. L. Beckham, K. M. Wyss, Y. Xie, E. A. McHugh, J. T. Li, P. A. Advincula, W. Chen, J. Lin, J. M. Tour, *Adv. Mater.* 2022, **34**, 2106506.

20 G. R. Surup, T. A. Pedersen, A. Chaldien, J. P. Beukes, M. Tangstad, *Processes* 2020, **8**, 2227.

21 L. G. Cançado, A. Jorio, E. H. M. Ferreira, F. Stavale, C. A. Achete, R. B. Capaz, M. V. O. Moutinho, A. Lombardo, T. S. Kulmala, A. C. Ferrari, *Nano Lett.* 2011, **11**, 3190.

22 W. Chen, C. Ge, J. T. Li, J. L. Beckham, Z. Yuan, K. M. Wyss, P. A. Advincula, L. Eddy, C. Kittrell, J. Chen, D. X. Luong, R. A. Carter, J. M. Tour, *ACS Nano* 2022, **16**, 6646.

23 P. Scotland, K. Wyss, L. Eddy, Y. Cheng, J. L. Beckham, Y. Chung, B. Wang, C. H. Choi, B. Deng, T. Si, Y.-Y. Shen, S. Zetterholm, C. Griggs, Y. Han, B. Tomson Mason, M. Wong, B. Yakobson, Y. Zhao, J. M. Tour, *ChemRxiv* 2023. DOI: 10.26434/chemrxiv-2023-6xj3m.

24 Y. Cheng, B. Deng, P. Scotland, L. Eddy, A. Hassan, B. Wang, K. J. Silva, B. Li, K. M. Wyss, M. G. Ucak-Astarlioglu, J. Chen, Q. Liu, T. Si, S. Xu, X. Gao, K. JeBailey, D. Jana, M. A. Torres, M. S. Wong, B. I. Yakobson, C. Griggs, M. A. McCary, Y. Zhao, J. M. Tour, *Nat. Commun*. 2024, 15.

25 H. Xie, N. Liu, Q. Zhang, H. Zhong, L. Guo, X. Zhao, D. Li, S. Liu, Z. Huang, A. D. Lele, A. H. Brozena, X. Wang, K. Song, S. Chen, Y. Yao, M. Chi, W. Xiong, J. Rao, M. Zhao, M. N. Shneider, J. Luo, J.-C. Zhao, Y. Ju, L. Hu, *Nature* 2023, **628**, 964.

26 X. Zhao, Y. Ando, Y. Liu, M. Jinno, T. Suzuki, *Phys. Rev. Lett.* 2003, **90**.

27 N. F. Andrade, T. L. Vasconcelos, C. P. Gouvea, B. S. Archanjo, C. A. Achete, Y. A. Kim, M. Endo, C. Fantini, M. S. Dresselhaus, A. G. Souza Filho, *Carbon* 2015, **90**, 172.

28 K. M. Wyss, D. X. Luong, J. M. Tour, *Adv. Mater.* 2022, **34**.

29 Col-Int Tech, 2024.

30 X. Zhao, Y. Ando, L.-C. Qin, H. Kataura, Y. Maniwa, R. Saito, *Chem. Phys. Lett.* 2002, **361**, 169.

31 S. Basirjafari, S. E. Khadem, R. Malekfar, *Curr. Appl. Phys.* 2013, **13**, 599.

32 J. Maultzsch, H. Telg, S. Reich, C. Thomsen, *Phys. Rev. B.* 2005, **72**.

33 R. B. Weisman, S. M. Bachilo, *Nano Lett.* 2003, **3**, 1235.

34 M. S. Dresselhaus, G. Dresselhaus, R. Saito, A. Jorio, *Phys. Rep.* 2005, **409**, 47.